Phase diagram of high-T_c superconductors: Influence of anisotropy and disorder

E. A. Jagla and C. A. Balseiro
Comisión Nacional de Energía Atómica, Centro Atómico Bariloche and Instituto Balseiro, 8400 San Carlos de Bariloche, Argentina
(Received 30 July 1996; revised manuscript received 30 September 1996)

We propose a phase diagram for the vortex structure of high-temperature superconductors which incorporates the effects of anisotropy and disorder. It is based on numerical simulations using the three-dimensional Josephson-junction array model. We support the results with an estimation of the internal energy and configurational entropy of the system. Our results give a unified picture of the behavior of the vortex lattice, from the very anisotropic $Bi_2Sr_2CaCu_2O_8$ to the less anisotropic $YBa_2Cu_3O_7$, and from the first-order melting ocurring in clean samples to the continuous transitions observed in samples with defects. [S0163-1829(97)04505-0]

I. INTRODUCTION

The phase diagram of high-temperature superconductors in the mixed state has provided an astonishingly broad field to workers in—among other fields—many body problems, polymer physics, low dimensional systems, critical phenomena, and statistical physics in general. The main reason for this situation is the great number of parameters that define the behavior of the vortex structure. On the other hand, the same abundance of parameters defining the system makes it difficult to find a unified description of all features observed in experiments. Some of the main parameters that define the behavior of the vortex structure are the external magnetic field H, temperature T, anisotropy η, and the disorder (which produces a non-homogeneous pinning potential for the vortices) that at this moment we loosely characterize by a parameter D. There are convincing explanations of the main characteristics of different sectors of this multidimensional phase diagram, such as the first-order melting of the vortex lattice in clean samples, the continuous melting of a glassy phase in disordered samples, or the existence of two different superconducting transitions (perpendicular and parallel to H) in some cases (for a review see Ref. 1). However, a unified description of the problem consistent with experiments, even in a qualitative level, is still lacking.

In this paper we propose a qualitative H-T-η-D phase diagram of high-T_c materials, that reproduces most of the available experimental results. Our approach is twofold: we use numerical simulation on the three-dimensional Josephson-junction array model to study the behavior of the system as a function of D and η, and show that the dependence on H can be deduced from a rescaling of D and η. The obtained phase diagram is then rederived using a phenomenological estimation of the free energy F of the system for different values of D and η. This estimation relies on the existence of two characteristic lengths ξ_c and ξ_{ab} parallel and perpendicular to the applied field H which are supposed to govern the behavior of the system. The minimizing of F with respect to ξ_c and ξ_{ab} allows one to obtain the $\xi_c(T)$ and $\xi_{ab}(T)$ functions, which in turn are used to detect the superconducting transitions.

The remainder of the paper is organized as follows. In the next section we present the results of the numerical simulations, and discuss the η-D phase diagram emerging from them. In Sec. III this phase diagram is qualitatively reobtained using a proposal for the free energy of the system. In Sec. IV we indicate that a change in the external magnetic field can be interpreted as a movement in the η-D plane, and so the H-T phase diagram for samples with different D and η can be obtained from the results of the previous sections. We also compare our results with those found in experimental studies. Finally in Sec. V, we summarize and conclude.

II. NUMERICAL SIMULATIONS

A. The model

Our numerical results are based on simulations performed on the three-dimensional (3D) Josephson-junction array (JJA) model on a stacked triangular network. The 3D JJA model has been previously used to show the first-order melting of the vortex lattice in clean systems.[2,3] Both thermodynamical and transport signatures of this first-order transition were obtained, in close relation to experimental results.[4] In addition, using the same model we have shown[5] that disorder can destroy the first-order transition, as observed in experiments.[6,7] The details of the model have been discussed elsewhere.[8,9] For completeness we present here briefly its main features.

The model consists on a mesh of Josephson junctions forming a stacked triangular network.[2] Each junction is modeled by an ideal Josephson junction with critical current I_c shunted by a normal resistance R_0 and its attached Johnson noise generator, which accounts for the effects of temperature. The equations for the 3D JJA model are

$$j^{ii'} = I_c \sin(\varphi^i - \varphi^{i'} - A^{ii'}) + \frac{\phi_0}{2\pi R_0} \frac{\partial(\varphi^i - \varphi^{i'})}{\partial t} + \vartheta^{ii'}(t), \tag{1}$$

$$\sum_{\{i'\}} j^{ii'} = j^i_{\text{ext}}, \tag{2}$$

where $\varphi^i(t)$ is the phase of the superconducting order parameter (vortices form in the system as singularities in the distribution of these phases), and ϕ_0 is the flux quantaum.

Equation (1) gives the current $j^{ii'}$ between nearest neighbor nodes i and i', $A^{ii'}$ is the vector potential of the external magnetic field, which will be always supposed to point in the crystallographic c direction (perpendicular to the triangular planes), and $\vartheta^{ii'}(t)$ is an uncorrelated Gaussian noise which incorporates the effects of temperature.

Equation (2) ensures the current conservation on each node, and $j^i_{\rm ext}$ is the external current applied at node i. Equations (1) and (2) are numerically integrated on time using a Runge-Kutta method suitable for stochastic systems. In the simulations we present here, we iterate the equations 2500 time steps for thermalization and then calculate observables during 10000 time steps at each temperature. The typical time step used is $\Delta t \simeq \tau_J$ ($\tau_J = \phi_0/2\pi R_0 I_c$). We checked that reducing the time step by a factor of 10 does not alter the results.

We systematically explore the case of anisotropic and disordered samples. Anisotropy is introduced by reducing the critical current of the c axis directed junctions by a factor η^2, and at the same time increasing the c axis normal resistance by the same factor. Disorder is introduced by randomly varying the critical current of the junctions through the lattice. As vortices gain energy when close to a low critical current region, the effect of randomizing the critical currents is to provide a nearly random pinning potential for vortices. We characterize the disorder by a parameter D which is defined as $D \equiv (I_c^{\max} - I_c^{\min})/(I_c^{\max} + I_c^{\min})$, where $I_c^{\max}$ and $I_c^{\min}$ are the maximum and minimum value of the critical current of the junctions through the sample. The probability distribution between $I_c^{\max}$ and $I_c^{\min}$ is taken flat. The results presented here were obtained for a single realization of disorder (the same for all values of η and D, up to the global amplitude). We have checked that other realizations do not change appreciably the results. This indicates that the system size used ($L_a \times L_b \times L_c = 18 \times 18 \times 18$ junctions, in all cases) is large enough for the system to be self-averaging.

We carried out simulations for $H = 1/6$ flux quanta per plaquette. This is the value used in Refs. 2 and 3. It produces a ground state (for a clean sample) which is commensurate with the subjacent triangular lattice, so no frustration effects are expected. Although the value 1/6 is rather large and effects of the substrate may be observable, we expect the physics of the problem to be qualitatively well described. In particular, we assume that for a clean sample the first-order melting observed in simulations is in fact the counterpart of the experimental observations.[4,7,10–12] It would be interesting to perform simulations at lower (commensurate) fields, such as 1/14 or 1/36. However, the sample size needed to minimize size effects make the computing time be exceedingly large.

We characterize the superconducting transitions by measuring the resistivity ρ of the sample when a small current is applied along the ab or c direction. Typically, an external current of 0.01 of the I_c in the corresponding direction is used. This value is small enough so as to test the linear resistivity of the sample. We will observe two well different behaviors of the resistivities as a function of temperature: in some cases resistivities have a jump from zero to a finite value at a given temperature. This jump in the resistivity corresponds (see the discussions below) to a first-order phase transition of the vortex lattice. In some other cases we will obtain that resistivities as a function of temperature smoothly depart from zero. We will refer to this behavior as a *continuous transition*. We do not claim at this moment about whether these continuous transitions are or are not real phase transitions, they can be crossovers as well. In Sec. V we present a discussion on this point. In addition, complementary results are presented, in which the superconducting coherence is characterized by the helicity modulus χ.[13] It measures the influence of a twist in the boundary conditions on the energy of the system, and has to be different from zero to indicate superconducting coherence. In the limit of infinite size, a finite value of χ (ρ) is equivalent to the vanishing of ρ (χ) in that direction. For finite samples a zone with both ρ and χ different from zero may appear due to finite size effects.

Boundary conditions (BC) deserve a comment. When calculating helicity modulus we use a system with periodic BC in all directions. However, in order to be able to apply a current to calculate resistivities we have to change the BC. To calculate the ab plane resistivity we simulate a system with open BC in the direction of the current, and periodic BC in the other two directions. When calculating c axis resistivity periodic boundary conditions are used in the a and b directions, and for the c direction we use an intermediate BC that we have called pseudoperiodic,[14,15] that allow to calculate the resistivity and at the same time reduces greatly the surface effects. In consequence, note that different magnitudes are calculated using different simulations, and a small difference in (for example) transition temperatures is likely to occur when comparing the results from ρ_c, ρ_{ab}, and χ.

B. Results

It turns out that the system has three very different kinds of behavior as a function of temperature depending on which value of disorder (D) and anisotropy (η) we are considering. We will first describe in detail typical points within the three different zones, and then show the complete η-D phase diagram.

We start by showing in Fig. 1 the results for a sample with $D = 0.3$ and $\eta^2 = 2$ as a function of temperature. Panel (a) shows the ab plane and c axis resistivity ρ_{ab} and ρ_c, panel (b) the corresponding values of the helicity modulus χ_{ab} and χ_c, and panel (c) the percolation probability P (see below). The behavior of the system in this case is typical of a first-order melting transition of the vortex lattice, as it was previously found in other works with $D = 0$:[2,3,5] helicity modulus both parallel and perpendicular to the field jump discontinuously to zero at the same temperature. The corresponding resistivities have also the same behavior. They are zero below the transition and have a finite value above it. The percolation probability shown in panel (c) is the probability that there exists a vortex path starting from one lateral side of the system and ending on the other side. We have shown in previous works[14,15] that the existence of these paths (i.e., the fact that $P \neq 0$) is a necessary condition to obtain finite c axis resistivity. The quantity P also jumps from zero to a finite value at the transition, indicating that this transition can be viewed as the passage from a solid crystalline phase (or a Bragg glass phase[16]) for $T < T_M$ to an entangled

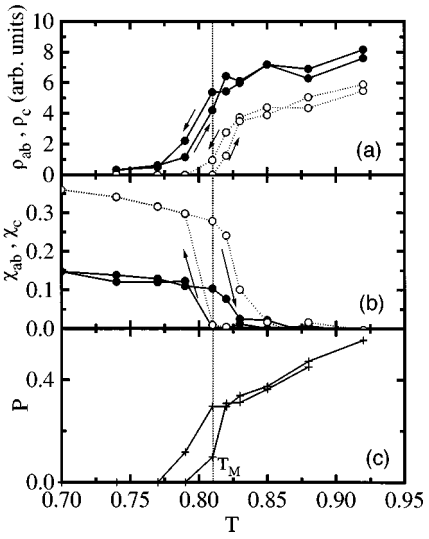

FIG. 1. (a) Resistivities ρ_{ab} (full symbols) and ρ_c (hollow symbols); (b) helicity modulus χ_{ab} (full symbols) and χ_c (hollow symbols); and (c) percolation probability P as a function of temperature for $\eta^2=2$ and $D=0.3$. Temperature is measured in units of the mean Josephson energy of the in-plane junctions. Magnetic field is $H=1/6$ quantum fluxes per plaquette. Results of successive cooling and heating are shown as indicated by the arrows. The approximate location of the melting temperature T_M is indicated.

liquid phase for $T>T_M$. All quantities show hysteresis around the transition typical of the first-order transition. The results just presented were obtained using finite D, so we conclude that the first-order transition is not restricted to the case $D=0$, but occurs in a finite region of the η-D plane.

When disorder is increased beyond certain limit, the first-order transition disappears.[6,7,5] Two different possibilities may occur. In Fig. 2 we show results similar to those of Fig. 1 but for $D=0.8$ and $\eta^2=0.5$. This corresponds to a highly disordered case, with low anisotropy. Superconducting transitions become continuous in this case, both when looking at

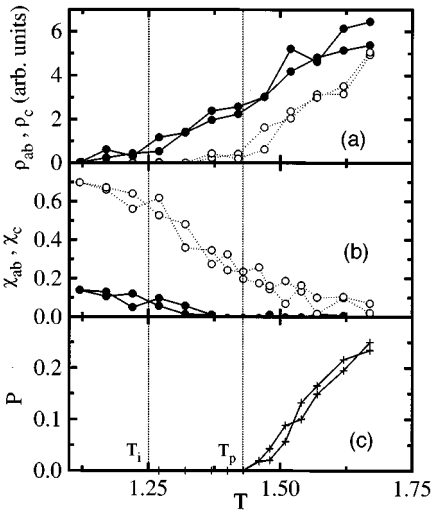

FIG. 2. Same as Fig. 1 but for a sample with anisotropy $\eta^2=0.5$ and $D=0.8$. No detectable hysteresis upon heating and cooling is observed. The approximate values of transition temperatures are indicated by the vertical lines.

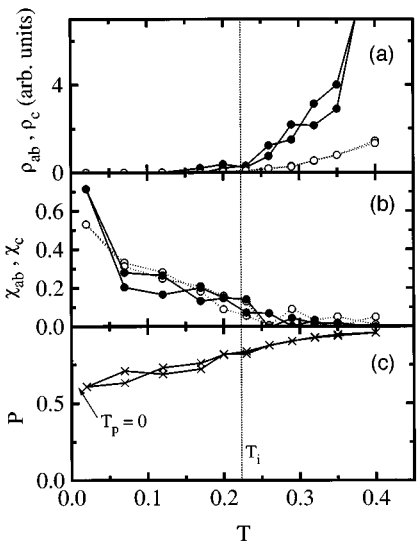

FIG. 3. Same as Fig. 2 but for a sample with anisotropy $\eta^2=20$ and $D=0.7$. Note that T_p has moved towards $T=0$.

them using resistivities or helicity modulus, and the parallel and perpendicular to field transitions occur at different temperatures. Note that, within numerical errors, hysteresis has disappeared. Perpendicular to field coherence is lost at a temperature T_i, whereas parallel to field coherence is lost at a temperature $T_p>T_i$.[14,15,17] At this temperature T_p both ρ_c and the percolation probability P become finite. For $T_i<T<T_p$ the system is in a dissipative state along the *ab* direction, but it is still superconducting along the *c* direction, and the vortex structure is that of a disentangled vortex liquid in this temperature range. At T_p a percolation phase transition occurs in the system.[14,15] This transition is triggered by the proliferation of vortex loops between planes.[18]

In Fig. 3 we show the results for $D=0.7$ and $\eta^2=20$. This corresponds to a highly disordered, highly anisotropic system. The most important feature of this case is that the percolation temperature is zero, i.e., the percolation probability P is finite even for $T\to 0$. This indicates that the vortex structure is in a highly disordered configuration and does not freeze into a disentangled lattice. Dissipation (both parallel and perpendicular to the field) appears only when temperature is increased beyond a finite value. We will keep the notation T_i for this value, as the temperature at which *ab* plane coherence is lost, and define T_p as the percolation temperature (at which P becomes different from zero), so in this case $T_p=0$, i.e., $T_p<T_i$. At the temperature T_i, both *ab* and *c* axis dissipation start to depart from zero in a very similar way,[19] in accordance with recent theoretical estimations.[20] Again no hysteresis is observed in this case either.

From the above discussion on Figs. 1, 2, and 3, the following picture emerges: at low disorder the vortex lattice melts through a first-order phase transition. When disorder increases this transition disappears, and the behavior depends on the anisotropy of the system. For low anisotropy in-plane and interplane coherence are lost at different temperatures T_i and $T_p>T_i$, and a disentangled vortex liquid phase exists for $T_i<T<T_p$. For highly anisotropic samples the percolation temperature T_p (in the sense of the temperature at which P becomes finite) moves to lower temperatures, indicating

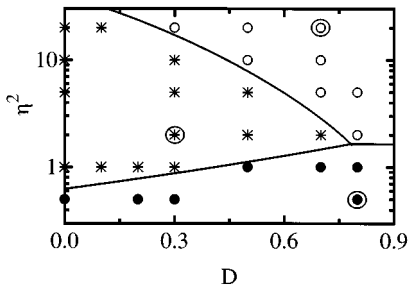

FIG. 4. Disorder-anisotropy phase diagram as obtained from the simulations. Stars indicate points where the melting transition is first order. Full circles are points where $T_i<T_p$, and hollow circles are points where $T_p<T_i$. The continuous lines are a sketch of the frontiers between the different zones. The encircled points are those analyzed in Figs. 1–3.

that the vortex structure freezes in an entangled configuration. Dissipation (in both directions) occurs for temperatures higher than a finite value T_i,[21] and we have $T_p<T_i$ in this case.

Having in mind these three qualitatively different behaviors, we have systematically searched the η-D space of parameters, and the results are shown in Fig. 4. Stars indicate points where the melting transition is first order. Full circles are points where $T_i<T_p$, and hollow circles are points where $T_p<T_i$. The points corresponding to Figs. 1–3 are shown encircled. The figure shows the three different zones discussed above. The continuous lines are a sketch of the frontiers between the different zones. The exact location of the border lines is difficult to determine precisely from the numerical simulations because different zones transform rather smoothly into each other when changing η and D, but the properties of the system within the different regions are physically different so as to guarantee the existence of such a frontier. In the next section we show that the main characteristics of this phase diagram can be derived from a simplified description of the vortex structure.

III. A SIMPLIFIED MODEL

We saw in the previous section that a single first-order transition is observed at low disorder, whereas two continuous transitions are obtained in disordered samples for low anisotropies. These features suggest that (at least for low anisotropies) the system may be described as having in general two different transitions: a depinning of rather independent vortices (ocurring at T_i), and a percolation transition (occurring at T_p) driven by the thermally generated loops. In certain cases they can merge onto a single first-order transition due to some kind of ''interaction.'' Here we show that this idea can be formulated more precisely by estimating the free energy of the system.

A. Free energy functional

To make this estimation we will consider first a single clean plane. We suppose that the thermodynamics of that plane can be phenomenologically described by a quantity ξ_{ab}, which is a correlation length: for distances shorter than ξ_{ab} the system has superconducting coherence, whereas this coherence is lost for distances larger than ξ_{ab}. The free energy functional $\mathcal{F}^{2D}$ of the plane has the form

$$\mathcal{F}^{2D}=E^{2D}(\xi_{ab})-TS^{2D}(\xi_{ab}) \tag{3}$$

(the thermodynamical free energy F is obtained by minimizing with respect to ξ_{ab}). For a system of L_c completely decoupled planes, we would have

$$\mathcal{F}^{3D}_{\eta\to\infty}=L_cE^{2D}(\xi_{ab})-TL_cS^{2D}(\xi_{ab}). \tag{4}$$

On the other hand, if the coupling between planes is infinite the vortices are rigid lines and we get

$$\mathcal{F}^{3D}_{\eta\to 0}=-(\alpha/\eta^2)L_c+L_cE^{2D}(\xi_{ab})-TS^{2D}(\xi_{ab}). \tag{5}$$

Note that in this case the entropy term does not have the factor L_c because giving the position of the vortices on one plane automatically determines the position of vortices in all other planes. The term $-(\alpha/\eta^2)L_c$ accounts for the energy gain due to the coupling of the planes, α being a numerical constant and η the anisotropy parameter defined before. In an intermediate situation ($0<\eta<\infty$) the system can be thought as formed by L_c/ξ_c layers (ξ_c is a number that satisfies $1<\xi_c<L_c$, see below). Within each layer the vortices are almost straight lines, whereas correlation is small between different layers. In this picture the free energy of the system is

$$\mathcal{F}^{3D}=-(\alpha/\eta^2)(L_c-L_c/\xi_c)+L_cE^{2D}(\xi_{ab}) -T(L_c/\xi_c)S^{2D}(\xi_{ab}). \tag{6}$$

In the first term, L_c-L_c/ξ_c is the number of sites along the c direction at which the system gains an energy α/η^2. The length ξ_c is roughly given by the mean distance between percolation paths along the c direction:[15] it takes a finite energy to bend a vortex in distances lower than ξ_c, however, this energy drops to zero for distances larger than ξ_c.

The previous estimation of the free energy of the system is too crude. In particular, in the form given by Eq. (6), it leads to some unphysical results. We must modify Eq. (6) slightly in order to obtain the correct behavior in some limiting cases. However, we will keep a fundamental property of Eq. (6) and make the guess that the entropy can be written for the real system as

$$S=f(\xi_c)S^{2D}(\xi_{ab}), \tag{7}$$

i.e., as a product of independent functions of ξ_c and ξ_{ab}, with $f(\xi_c)$ and $S^{2D}(\xi_{ab})$ two yet unknown functions. The basic assumption contained in Eq. (7) is the following: if the value of ξ_c is kept fixed, then the system behaves as a two-dimensional system with a renormalized temperature. Al-

though this assumption cannot be fully justified *a priori*, it is a natural starting point, and gives sensible results as we will show soon.

We still have to add a term to the free energy which accounts for the effect of impurities. Impurities decrease the energy of the system when vortices pin to them. If pinning is uncorrelated the energy gain due to pinning becomes lower when the vortex positions are more correlated. So we add a term to the free energy that increases the energy of the system when ξ_{ab} and ξ_c increase. The most simple term of this type is of the form $D\xi_{ab}\xi_c$. Finally, the free energy functional of the system $\mathcal{F}(\xi_{ab},\xi_c)$ (dropping an irrelevant constant term) is

$$\mathcal{F}(\xi_{ab},\xi_c)=(\alpha/\eta^2)L_c/\xi_c+L_cE^{2D}(\xi_{ab})-Tf(\xi_c)S^{2D}(\xi_{ab}) +D\xi_{ab}\xi_c. \tag{8}$$

The true expressions for the functions f, E^{2D}, and S^{2D} are difficult to establish. However, it is not our aim to give a complete quantitative description of the free energy of the system but only a qualitative description of the phase diagram. We will only ask the functions f, E^{2D}, and S^{2D} to reproduce some known limiting cases: if ξ_c (ξ_{ab}) is kept fixed we expect the value of $\xi_{ab}(T)$ ($\xi_c(T)$) obtained by minimizing $\mathcal{F}$, to be smoothly dependent on temperature. This corresponds to the absence of first-order transitions in the dynamics of a single plane (a single vortex line).[22] However, when $\mathcal{F}$ is minimized with respect to *both* ξ_c and ξ_{ab} a *discontinuity* in $\xi_c(T)$ and $\xi_{ab}(T)$ can appear, as we show below.

Just to give an example we use for the function f the form $f=\gamma\ln(L_c/\xi_c)+1$. The term $\gamma\ln(L_c/\xi_c)$ (γ is a numerical constant) is proportional to the entropy of a single (isolated) vortex line. The constant added assures that the two-dimensional limiting case of rigid sticks is reobtained when $L_c=\xi_c$. In addition, we will take for the functions E^{2D} and S^{2D} the form $E^{2D}=L_{ab}/\xi_{ab}$ and $S^{2D}=\gamma\ln(L_{ab}/\xi_{ab})+1$, in such a way that we obtain a form for the free energy functional that is (unphysically) symmetric (for $\alpha/\eta^2=1$) between *ab* and *c* directions. We have tested other forms of the functions f, E^{2D} and S^{2D} (giving the same limiting behavior discussed above) and found results qualitatively similar to those shown here.

We arrive to our final working expression of the free energy functional (we will measure ξ_{ab} and ξ_c in units of L_{ab} and L_c, respectively, take $\alpha=1$ by rescaling η, and also rescale D)

$$\mathcal{F}(\xi_{ab},\xi_c)=1/\eta^2\xi_c+1/\xi_{ab}-T[\gamma\ln(1/\xi_c)+1] \times[\gamma\ln(1/\xi_{ab})+1]+D\xi_{ab}\xi_c. \tag{9}$$

The thermodynamical free energy F is obtained by minimizing with respect to ξ_{ab} and ξ_c:

$$F(T)=\min_{0\le\xi_{ab}\le1}\ \min_{0\le\xi_c\le1}\ \mathcal{F}(\xi_{ab},\xi_c). \tag{10}$$

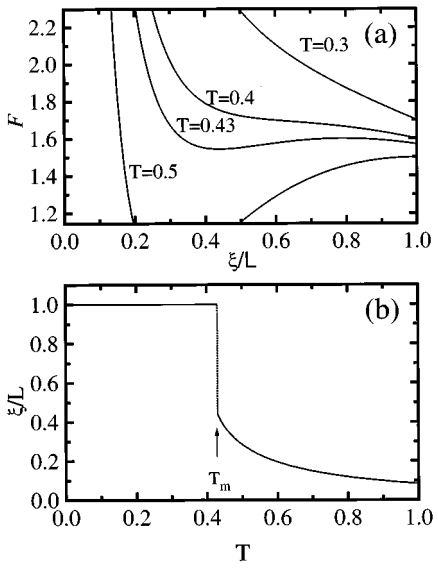

FIG. 5. (a) Free energy functional as a function of correlation length ξ for different temperatures with $D=0$, and $\gamma=2$. (b) Correlation length as a function of temperature obtained as the minima of the curves in (a).

We stress again we do not claim expression (9) is a good detailed description of the free energy of the system, but only a expression [whose main characteristic is given by Eq. (7)], that will help us to understand different sectors of the η-D phase diagram of high-T_c's.

B. Results

We present now the results obtained by minimizing the free energy functional given by expression (9). When doing this minimization we obtain the free energy F and the lengths ξ_{ab} and ξ_c as a function of temperature. A first-order transition is identified as a discontinuous jump in the values of the correlation lengths ξ_{ab} and ξ_c at the same temperature from 1 (long range correlation) to a lower value (finite range correlation). If this is not the case, the dependence of ξ_{ab} and ξ_c with temperature gives a clue on how the superconducting coherence is lost when raising temperature. However, in this case the identification of a phase transition is not simple, and we can only identify temperature ranges where coherence along *c* or *ab* directions is high or low.

Let us start with the case $D=0$ and $\eta=1$ (note that we are using a renormalized anisotropy parameter, so $\eta=1$ does not imply necessarily an isotropic system). In this case Eq. (9) is symmetric in ξ_{ab} and ξ_c, and in fact the minima of $\mathcal{F}$ are on the line $\xi_{ab}=\xi_c\equiv\xi$, so in Fig. 5 we plot the function $\mathcal{F}(\xi,\xi)$ for different values of the temperature. We see that when $T\to0$ the minimum free energy state corresponds to the maximum possible value of ξ, i.e., the system is in the ordered state. When temperature increases a *first-order* transition to a disordered state occurs. This is also seen from the behavior of ξ as a function of temperature, as depicted in Fig. 5(b). Thus we see that the coupling of two continuous transitions [through the entropy term in Eq. (9)] can merge them onto a single one, which is first order. In fact, such sort

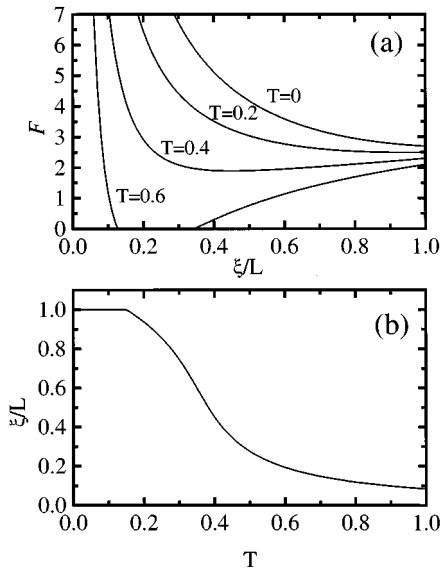

FIG. 6. Same as Fig. 4 but with $D=0.7$.

of mechanism has been previously proposed to occur in other cases, such as two-dimensional melting, in which the continuous dislocation-unbinding and disclination-unbinding transitions of the Kosterlitsz-Thouless-Halperin-Nelson-Young melting theory[23,24] can collapse onto a first-order melting transition.[24,25]

If disorder is present in the system it will tend to destroy the melting transition. In Fig. 6 we show results as those of Fig. 5 but for a value of $D=0.7$. As we see the jumps in ξ_{ab} and ξ_c have disappeared, indicating that the transition is not first order. If the anisotropy had been chosen different from one, then the temperature at which ξ_{ab} and ξ_c take a given value would have been different. Although we cannot characterize from our simplified model a phase transition when ξ_{ab} and ξ_c are continuous functions of temperature, it is tempting to say that if ξ_{ab} (ξ_c) drops to zero at lower temperature than ξ_c (ξ_{ab}), then we are in a sector of the phase diagram where $T_i<T_p$ ($T_p<T_i$).[26] In this way we generate the phase diagram depicted in Fig. 7. As indicated, it is qualitatively similar to the one obtained from the numerical simulation, and it gives support *a posteriori* to the proposal of an entropy of the system of the form given by Eq. (7).

Some characteristics of this phase diagram can be analyzed in simple terms. For example, when $\eta\rightarrow\infty$, the system is a set of decoupled planes, and no first-order transition is obtained for any value of D.[22] When $\eta\rightarrow 0$ vortices are rigid lines and in fact effectively two-dimensional, so a first-order transition is not obtained in this case either. These limiting cases give some insight on the form of the border between first order and continuous transitions in Figs. 4 and 7. There is an optimum value of the anisotropy, at which the first-order transition persists up to a highest value of disorder. This optimum value depends on the thickness of the sample. In fact, as we discussed in a previous work,[15] in samples with low anisotropy the temperature T_p logaritmically *decreases* when the thickness of the sample increases. This means that in Fig. 4 the border between the zones with $T_i>T_p$ and $T_p>T_i$ moves to lower values of η. It is thus

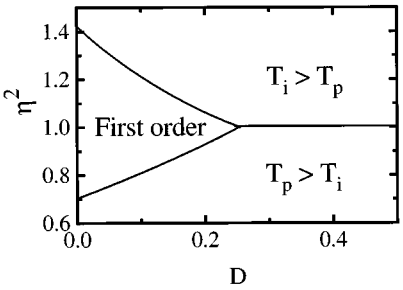

FIG. 7. Disorder-anisotropy phase diagram as obtained by minimizing the free energy functional (see text for explanation).

likely that the optimum value of η for the occurrence of the first-order transition also decreases with sample thickness.

IV. MAGNETIC FIELD DEPENDENCE AND COMPARISON WITH EXPERIMENTS

Having discussed the η-D phase diagram for a fixed magnetic field H, we turn now to the discussion of the dependence on H. From the numerical point of view the direct approach would be to do simulations at different fields. However, as we discussed above, to reduce the magnetic field to other commensurate values would require exceedingly large computing time. Fortunately, there are arguments that suggest that a change of H can be mapped onto a change of D and η.

The scaling combination between magnetic field and anisotropy has been given by Chen and Teitel.[27] We generalize here the argument to include the disorder parameter D. Our dimensionless temperature (measured in units of the mean Josephson energy of the in-plane junctions) can be only a function of the other dimensionless parameters of the system. These are D, H, and η. These parameters have different dependences on the coherence length ξ_0. If we identify the discretization parameter in the *ab* plane with a distance of the order of the coherence length ξ_0, then the critical current of the Josephson junctions along the *c* direction $I_c^{\perp}$ is proportional to ξ_0^2, so the anisotropy parameter η $[\sim(I_c^{\perp})^{-1/2}]$ behaves as ξ_0^{-1}. On the other hand, our dimensionless magnetic field H is given in terms of the real external magnetic field H_0 by the expression $H=H_0\xi_0^2/\phi_0$. For the parameter D, we note that D is proportional to the amplitude of the pinning potential. A vortex averages this random function on an area $\sim\xi_0^2$. Considering the case of random (uncorrelated) pinning we find that D depends on ξ_0 as $D\sim\xi_0^{-1}$. Since we are ignoring details of the vortex cores, we expect the properties of the system to depend only on the ξ_0-independent quantities $\eta^2 H$ and $D^2 H$.

We conclude that we can obtain the behavior of the system as a function of magnetic field from the results of Fig. 4 on lines with constant D/η. A sketch of the different possibilities is shown in Fig. 8. The general prediction from Fig. 4 is depicted in Fig. 8(a). The scales on the axis as well as the extent of the first-order transition depend on the particular value of D/η. This general picture has to be modified at very low fields. In fact, a minimum crossover field[14] (given essentially as the field at which the vortex lattice parameter

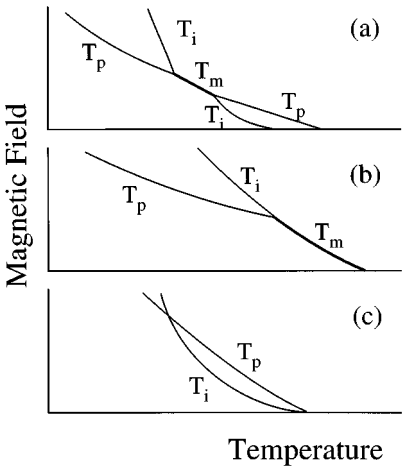

FIG. 8. Qualitative sketch of the H-T phase diagram for different values of D/η. (a) General form. (b) D/η small. (c) D/η high.

matches the thickness of the sample) exists, below which T_i and T_p are essentially the same (this is because in this case there are so few vortices in the sample that the transition is entirely due to thermally generated vortex loops). Different possibilities are depicted in Figs. 8(b) and 8(c). They correspond to different ranges of values of D/η. Figure 8(b) corresponds to D/η small, so Fig. 4 predicts $T_p<T_i$ at high fields, and a first-order zone at intermediate and low fields. This phase diagram corresponds to that experimentally obtained for $Bi_2Sr_2CaCu_2O$,[28] which in fact has the largest value of η, and even to the case of clean $YBa_2Cu_3O_7$,[29] which has a very low D. Figure 8(c) shows the expected phase diagram for samples with a high value of D/η. At low fields T_i is lower than T_p, whereas at high fields a crossover to a zone with $T_i>T_p$ is possible. No first-order zone is shown because a curve defined by a high value of D/η in Fig. 4 does not pass through the first-order zone. The low field part of this phase diagram corresponds to the one obtained for $YBa_2Cu_3O_7$ samples with defects.[30] The crossover to a case with $T_i<T_p$ has not been observed, presumably because of the high fields needed.

As we indicated above, when $T_i<T_p$ superconducting coherence is lost along the *ab* plane at lower temperatures than along the *c* axis. For $T_i<T<T_p$ finite resistance within the planes and zero resistance in the *c* direction is observed. When $T_i>T_p$ and in the case that $T_i>T>T_p$ we potentially expect finite resistance in the *c* direction and zero resistance within the planes. This has turned out to be difficult to find, both experimentally[31] and in our simulations. The resistance seems rather to go to zero at the same temperature T_i in all directions.[21] This is due to the fact that vortex paths crossing the sample for $T>T_p$ are pinned to the *ab* planes as long as $T<T_i$, preventing their movement (and thus dissipation). However, it is worth noting that some other experimental measurements of coherence (ac magnetization) indicate[32] that in fact, *c*-axis coherence is lost at lower temperatures than in-plane coherence for the case of $Bi_2Sr_2CaCu_2O$.

The transitions observed in our simulations are of different character, and we want to discuss the point a bit further. The first-order transition is the easiest to characterize numerically. Although we do not show all the results, we observed that when the resistivity has a jump other indicators point to a first-order phase transition, as for example the energy histogram of the system, which has two peaks right at the transition temperature, indicating two coexisting phases with an energy barrier separating them.[33,2] The continuous transitions are more difficult to characterize. The transition at T_i for samples with low anisotropy *is not* a phase transition in our model. In fact, it is a crossover due to thermal depinning of rather independent vortices.[9] However, in a real sample it may correspond to the vortex glass transition, depending on the strength of the disorder.[34] When $T_p>T_i$, we have previously characterized the transition at T_p as a percolation phase transition of the vortex structure perpendicularly to the applied field.[15] In the thermodynamic limit for L_{ab} ($L_{ab}\to\infty$) the system does not have any vortex line running perpendicularly to the applied field for $T<T_p$, whereas for $T>T_p$ these paths extend all over the *ab* plane with probability one. In Refs. 14 and 15 we showed numerical evidence suggesting that this transition is a second-order phase transition and gave its critical exponents as found from simulations.

V. SUMMARY AND CONCLUSIONS

In this paper we present numerical evidence that supports an anisotropy-disorder phase diagram of the vortex structure of high-T_c's with the following characteristics: For clean samples the vortex lattice melts through a first-order phase transition for a wide range of anisotropies. When disorder is included the behavior of the system is strongly dependent of the anisotropy. For low anisotropies the in-plane coherence is lost at a temperature T_i lower than the temperature T_p at which interplane coherence is lost, and a zone of disentangled vortex lines is observed for $T_i<T<T_p$. For highly anisotropic samples the superconducting coherence as deduced from simulations of the resistivity is lost at the same temperature T_i within the planes and perpendicularly to the planes. However, in this case the vortex structure percolates at a temperature T_p well below T_i. In this case the system for $T_p<T<T_i$ is in an ''entangled solid'' phase. These features are also obtained from an estimation of the free energy of the system which is mainly based on a proposal for the entropy of the system [Eq. (7)]. We showed that the magnetic field-temperature behavior of the system can be deduced from results obtained from a fixed magnetic field provided the anisotropy and disorder present in the system are properly rescaled.

Our results present, in a unified way, different characteristics of the vortex structure that had been previously found in partial studies. The analysis is in agreement with a variety of experiments performed on different materials with a broad range of parameters such as disorder, anisotropy, and magnetic field. It could prove to be useful to find a more solid base of our proposal for the free energy of the system—that we showed is qualitatively good—in order to obtain more detailed analytical results.

ACKNOWLEDGMENTS

We acknowledge helpful discussions with D. López, E. F. Righi, and F. de la Cruz. E.A.J. acknowledges financial support by CONICET. C.A.B. was partially supported by CONICET.

[1] G. Blatter *et al.*, Rev. Mod. Phys. **66**, 1125 (1994).
[2] R. E. Hetzel, A. Sudbo, and D. A. Huse, Phys. Rev. Lett. **69**, 518 (1992).
[3] D. Domínguez, N. G. Jensen, and A. R. Bishop, Phys. Rev. Lett. **75**, 4670 (1995).
[4] H. Safar *et al.*, Phys. Rev. Lett. **69**, 824 (1992); W. K. Kwok *et al.*, *ibid.* **72**, 1092 (1994).
[5] E. A. Jagla and C. A. Balseiro, Phys. Rev. Lett. **77**, 1588 (1996).
[6] J. A. Fendrich *et al.*, Phys. Rev. Lett. **74**, 1210 (1995).
[7] D. López *et al.*, Phys. Rev. Lett. **76**, 4034 (1996).
[8] D. Domínguez and J. V. José, Phys. Rev. B **48**, 13717 (1993).
[9] E. A. Jagla and C. A. Balseiro, Phys. Rev. B **52**, 4494 (1995).
[10] H. Pastoriza *et al.*, Phys. Rev. Lett. **72**, 2951 (1994).
[11] E. Zeldov *et al.*, Nature (London) **375**, 373 (1995).
[12] D. López *et al.*, Phys. Rev. B **53**, 8895 (1996).
[13] M. E. Fisher, N. M. Barber, and D. Jasnow, Phys. Rev. A **8**, 1111 (1972); Y. H. Li and S. Teitel, Phys. Rev. B **47**, 359 (1993).
[14] E. A. Jagla and C. A. Balseiro, Phys. Rev. B **53**, 538 (1996).
[15] E. A. Jagla and C. A. Balseiro, Phys. Rev. B **53**, 15 305 (1996).
[16] T. Giamarchi and P. Le Doussal, Phys. Rev. Lett. **72**, 1530 (1994); Phys. Rev. B **52**, 1242 (1995).
[17] Although the exact values of T_i and T_p depend on whether we determine them from ρ or χ, we found in all cases that the fact that T_i is lower than T_p or not is independent of this, and this is the crucial point to be able to construct the phase diagram of Fig. 4, which is based on relations between T_i and T_p, and not on the exact values of these temperatures.
[18] Y. -H. Li and S. Teitel, Phys. Rev. B **49**, 4136 (1994).
[19] F. Laguna, E. A. Jagla, and C. A. Balseiro (unpublished).
[20] A. Koshelev, Phys. Rev. Lett. **76**, 1340 (1996)
[21] In Ref. 15 we showed some results on anisotropic cubic lattices where a zone with $\rho_c \neq 0$ and $\rho_{ab}=0$ was observed. This dissipation is probably due to the movement of percolation paths lying entirely between two consecutive planes, thus being unaffected by the pinning of the *ab* planes. We did not observe clearly the same effect on triangular lattices up to now.
[22] A first-order transition has been reported for a single plane [W. Yu, Ph.D. thesis, Ohio State University, 1994, and also M. Franz and S. Teitel, Phys. Rev. B **51**, 6551 (1995)]. However, this transition is very weakly first order. A strong first-order transition as that of Fig. 1 is observed only in the case of three-dimensional systems and in fact, only when the thickness is higher than a minimum value [see Ref. 5 and also G. Carneiro, Phys. Rev. Lett. **75**, 521 (1995)]. Since we are interested in the strong first-order transition appearing in three-dimensional samples, we will refer to a single plane as having a continuous transition (see also the discussion of Fig. 1 in Ref. 5).
[23] J. M. Kosterlitz and D. J. Thouless, L. Phys. C **6**, 1181 (1973); A. P. Young, Phys. Rev. B **19**, 1855 (1978).
[24] B. I. Halperin and D. R. Nelson, Phys. Rev. Lett. **41**, 121 (1978); D. R. Nelson and B. I. Halperin, Phys. Rev. B **19**, 2457 (1978).
[25] H. Kleinert, *Gauge Fields in Condensed Matter* (World Scientific, Singapore, 1989).
[26] Since we defined ξ_c as related to the distance between percolation path, the case $\xi_c=1$ has to be associated to a percolation probability P equal to zero, i.e., the temperature T_p as defined here corresponds to the same magnitude defined in the previous section.
[27] T. Chen and S. Teitel (unpublished).
[28] F. de la Cruz *et al.*, Physica B **197**, 596 (1994).
[29] D. López, E. F. Righi, S. Grigera, and F. de la Cruz (private communication).
[30] F. de la Cruz, D. López, and G. Nieva, Philos. Mag. B **70**, 773 (1994).
[31] G. Briceño, M. Crommie, and A. Zettl, Phys. Rev. Lett. **66**, 2164 (1991).
[32] A. Arribere *et al.*, Phys. Rev. B **48**, 7486 (1993).
[33] J. Lee and J. M. Kosterlitz, Phys. Rev. Lett. **65**, 137 (1990).
[34] M. I. J. Probert and A. I. M. Rae, Phys. Rev. Lett. **75**, 1835 (1995).